Materials Advances

ROYAL SOCIETY OF CHEMISTRY

PAPER

View Article Online
View Journal | View Issue

Cite this: *Mater. Adv.*, 2026, 7, 5075

Epoxidized camelina oil as a renewable plasticizer to develop highly toughened and flexible polylactic acid films

Muhammad Arshad,[a] Malik Hassan,[ab] Arturo Rodriguez-Uribe,[a] Amar K. Mohanty *[ab] and Manjusri Misra *[ab]

This study investigates the influence of epoxidized camelina oil (ECO) as a plasticizer on the thermal behavior, mechanical performance, and morphological features of polylactic acid (PLA). ECO was incorporated into PLA at 5%, 10%, and 15% by weight, and its effects on elongation at break, impact resistance, modulus, and fracture behavior were evaluated. Nuclear magnetic resonance (NMR) spectroscopy confirmed the successful epoxidation of camelina oil through the disappearance of olefinic proton signals and the appearance of oxirane group signals, validating the high degree of functionalization. Similarly, Fourier-transform infrared (FTIR) spectroscopy confirmed the conversion of double bonds into epoxide groups through the appearance of oxirane peaks and the disappearance of –C=C–H stretching vibrations, along with shifts in PLA carbonyl peaks, indicating hydrogen bonding and strong intermolecular interactions. Mechanical testing showed that addition of 10% ECO significantly enhanced the material properties, with a 1680% increase in elongation at break and a 24% improvement in impact strength compared to neat PLA, indicating substantial improvements in flexibility and toughness. SEM micrographs of tensile and impact fracture surfaces confirmed the transition from brittle to ductile failure with increasing ECO content, showing rougher surfaces, localized plastic deformation, and reduced crack propagation. Thermal analysis demonstrated a reduction in the glass transition temperature with ECO addition, further validating its role as a plasticizer. This study demonstrates that ECO effectively tailors the properties of PLA, making it suitable for applications requiring improved ductility, toughness, and energy absorption, such as packaging and biomedical materials.

Received 23rd January 2026,
Accepted 25th February 2026

DOI: 10.1039/d6ma00115g

rsc.li/materials-advances

1. Introduction

In recent years, increased concern about climate change has been raised by governments, industries, and communities due to the higher rate of greenhouse gas emissions resulting from non-renewable waste disposal, emphasizing the replacement with renewable resources or bio-based materials.[1–3] Polylactic acid (PLA) is an attractive "green" alternative to petroleum-based plastics due to its renewable origin from the fermentation of agricultural carbohydrates. With similar performance properties to many commodity plastics, PLA has been found to degrade within 3–6 months under composting conditions. In order for a polymer to be considered compostable, greater than 90% weight loss must occur within 180 days, the degradation process should not produce any toxic by-products, and the final compost should be able to support plant growth.[4] PLA meets these criteria, making it an ideal candidate to reduce environmental impact. Due to its biodegradability, high mechanical strength and biocompatibility, it is an attractive candidate in numerous industrial applications such as textiles, packaging, biomedical materials and many others.[5–7] However, its low toughness and elongation at break limit its potential applications to serve as a substitute for fossil-derived materials and products.[8,9] Hence, improving the toughness and ductility of PLA is an ultimate requirement for its application in the development of bio-based materials. In this regard, numerous techniques and strategies such as copolymerization, blending with other polymers, PLA modification using plasticizers, and incorporating fillers have been employed to toughen PLA.[10,11]

Plasticizers play a dual role in polymer systems: they not only improve processability but also enhance the flexibility and ductility of rigid, glassy polymers. For PLA, an ideal plasticizer should effectively lower its glass transition temperature (T_g), be biodegradable, non-toxic, and non-volatile, and exhibit minimal leaching or migration over time.[12–14] The efficiency of a plasticizer is typically assessed by its ability to reduce T_g and

[a] *Bioproducts Discovery and Development Centre, Department of Plant Agriculture, University of Guelph, Crop Science Building, Guelph, Ontario, N1G 2W1, Canada. E-mail: mohanty@uoguelph.ca, mmisra@uoguelph.ca*
[b] *Department of Interdisciplinary Engineering, College of Engineering, University of Guelph, Thornbrough Building, Guelph, Ontario, N1G 2W1, Canada*

improve tensile toughness, which depends on its compatibility with the polymer matrix, molecular weight, and loading concentration.[15–17]

Plant oils being renewable, non-toxic, inexpensive, abundant, and biodegradable[18,19] are considered suitable green feedstocks and alternatives to petroleum based additives/plasticizers to serve as a toughness modifier for PLA. However, different derivatized forms of vegetable oils such as epoxidized palm oil and soybean,[20–23] maleinized linseed, hempseed, and cotton seed oil,[24–26] and acrylated epoxidized soybean oil[21] have been reported as plasticizers to improve PLA toughness. However, most vegetable oil derivatives have not achieved the desired toughness due to their incompatibility with PLA.[27,28]

Camelina oil presents several advantages that make it a promising precursor for renewable plasticizers. It is a non-edible oilseed crop that grows well on marginal land with low fertilizer and water requirements, which reduces competition with food resources and improves its overall sustainability profile.[29] The oil contains a high proportion of polyunsaturated fatty acids, typically 50%, with alpha-linolenic acid (30–40%) as the dominant component.[30] This high level of unsaturation provides a large number of reactive carbon–carbon double bonds, which enables efficient conversion to oxirane rings during epoxidation and results in a high epoxy group density per gram of product. A high epoxy density strengthens the interaction between the modified oil and polar polymer matrices such as PLA and improves plasticization performance. Previous studies have shown that epoxidized oils with higher level of unsaturation produce more effective toughening and flexibility improvements in biodegradable polymers because of their higher reactivity and stronger secondary interactions with the polymer chains. These characteristics highlight the potential of camelina oil as a suitable and sustainable feedstock for the development of renewable plasticizers.

In this study, camelina oil, sourced from "*Camelina sativa*", a non-food oilseed crop, was epoxidized and utilized as a plasticizer to enhance the ductility and toughness of PLA. Camelina oil with high unsaturated content (90%) was epoxidized through treatment with hydrogen peroxide and formic acid, using a catalyst to facilitate the reaction.[31,32] The developed epoxidized camelina oil (ECO) was characterized with Fourier transform infrared (FTIR) and nuclear magnetic resonance (NMR) and used as a plasticizer for PLA. Various ratios of ECO (5, 10 and 15%) as a plasticizer were blended with PLA using injection molding. The fabricated blends of epoxidized camelina oil in PLA (ECO–PLA) were investigated for thermal and mechanical properties to study the impact of the plasticizer on the improvement in toughness and ductility of PLA.

2. Materials and methods

2.1. Materials

Camelina oil was obtained from Smart Earth Company (Saskatoon, Canada). Polylactic acid (PLA) (Ingeo 3251D) was supplied by NatureWorks. It has a melting temperature in the range of 155 °C to 170 °C and a melt flow rate, at 190 °C under a load of 2.16 kg, of 30 to 40 g/10 min. Additional chemicals, including Amberlite-IR120 ion exchange resin (hydrogen form, Fluka, St. Louis, MO, USA), formic acid (98%, EMD Millipore), hydrogen peroxide (30 wt% in water), toluene (≥99.5%), sodium chloride (≥99.0%), and anhydrous magnesium sulfate (≥97%) were purchased from Sigma Aldrich and used without further modification.

2.2. Epoxidation of camelina oil (ECO)

The camelina oil was epoxidized using a method adapted from a previously reported procedure.[33] Briefly, 200 g of camelina oil, 20 g of amberlite ion exchange resin–H^+, and 33.3 g of formic acid were taken and dissolved in 150 mL of toluene. 200 mL of H_2O_2 solution (30 wt%) was added dropwise into the flask in about 20 minutes. Caution should be taken due to the highly exothermic nature of the reaction. After the addition of H_2O_2, the temperature was maintained at 60 °C, under continuous heating. The reaction was completed within 3 hours as confirmed by FTIR. Upon completion, the reaction mixture was cooled down to room temperature, and the resin was removed by filtration. The organic layer was washed three times with 750 mL of water, and 100 mL of brine was added to separate any emulsions. The washed organic layer was dried using anhydrous magnesium sulfate, filtered, and evaporated using rotary vapor. The process yielded a light-yellow liquid product weighing 201 g.

In this study, Amberlite IR120 in the hydrogen form was selected as the catalyst for the epoxidation of camelina oil because it provides strong protonic acidity, high catalytic efficiency, and convenient handling during the Prilezhaev type epoxidation reaction. The solid resin promotes the *in situ* formation of performic acid from formic acid and hydrogen peroxide, which then reacts with unsaturated bonds in camelina oil to form oxirane rings. Unlike liquid mineral acids such as sulfuric acid, Amberlite does not create corrosion concerns, does not require neutralization after the reaction, and reduces the formation of unwanted side products, including excessive ring opening or oxidative degradation. The heterogeneous nature of the resin allows simple removal by filtration and enables reuse in subsequent reactions, which improves the sustainability of the process. These advantages, combined with reliable catalytic activity and minimal environmental impact, make Amberlite IR120 an effective and practical catalyst for producing highly epoxidized camelina oil.

2.3. Fabrication of ECO–PLA blends

The PLA pellets and ECO were subjected to drying in an oven at 80 °C overnight to achieve a moisture content below 0.1%. The blends of PLA and ECO were prepared using a DSM Xplore 15 mL laboratory-scale microcompounder (Xplore Instruments BV, The Netherlands), equipped with co-rotating twin screws of 150 mm in length and an aspect ratio (L/D) of 18, and a barrel comprising three independently controlled heating zones. For extrusion, PLA and ECO (5 wt%, 10 wt%, and 15 wt%) were manually mixed and directly fed into the barrel. The compounding

was performed at a processing temperature of 180 °C and a screw speed of 100 rpm. The materials were retained within the barrel for a fixed residence time of 2 minutes to ensure complete melt homogenization before being transferred directly into the injection molding chamber, which was set at 40 °C. The prepared blends were labeled as 5% ECO–PLA, 10% ECO–PLA, and 15% ECO–PLA, respectively. A neat PLA control sample (without ECO) was also processed under identical conditions for comparison.

3. Characterization techniques

3.1. Fourier-transform infrared (FTIR) analysis

FTIR analysis was performed on the prepared samples using a Nicolet 6700 ATR-FTIR spectrometer (ThermoScientific, USA). The spectra were recorded at a resolution of 4 cm^{-1} across a wavenumber range of 500–4000 cm^{-1}, with an average of 64 scans per spectrum.

3.2. Nuclear magnetic resonance (NMR) analysis

NMR spectra were recorded using a Bruker AVANCE III spectrometer operating at 600 MHz, equipped with a 5-mm TCI cryoprobe. Deuterated chloroform ($CDCl_3$) was used as the solvent for all experiments.

3.3. Thermal analysis

Differential scanning calorimetry (DSC) was performed using a Q200 system (TA Instruments, New Castle, DE, USA), which included a cooling system, to determine the melting, crystallization, and glass transition temperatures of the samples. Specimens weighing 5–10 mg were sealed in aluminum pans for the analysis. The procedure commenced with an initial heating cycle from −70 °C to 200 °C at a heating rate of 10 °C min^{-1}, followed by an isothermal hold for 2 minutes at 200 °C. This was followed by a cooling cycle to cool the sample to −70 °C from 200 °C at a rate of 5 °C min^{-1}, with an additional isothermal hold at −70 °C for 2 minutes. Finally, a second heating cycle was carried out under the same conditions as the first heating cycle.

Thermogravimetric analysis (TGA) was performed using a Q500 thermogravimetric analyzer (TA Instruments, Delaware, USA) to examine the thermal degradation behavior of the samples. Specimens with a mass of 10–20 mg were heated from room temperature to 600 °C at a rate of 10 °C min^{-1}, while maintaining a nitrogen flow of 60 mL min^{-1}.

3.4. Dynamic mechanical analysis (DMA)

DMA was performed using a Q800 dynamic mechanical analyzer (TA Instruments, USA) to evaluate the viscoelastic properties of neat PLA and ECO–PLA blends. Rectangular specimens (35 mm × 12 mm × 3 mm) were tested using a dual cantilever clamp in multi-frequency strain mode. The analysis was conducted at a fixed frequency of 1 Hz and a displacement amplitude of 20 μm, ensuring that measurements were taken within the linear viscoelastic region (LVR). The test began with temperature equilibration at −35 °C, followed by heating to 120 °C at a rate of 3 °C min^{-1} in multi-frequency strain mode. Throughout the test, the storage modulus (E'), loss modulus (E''), and damping factor ($\tan\delta$) were recorded. The glass transition temperature (T_g) was determined from the peak of the $\tan\delta$ curve, and the effect of ECO concentration on molecular mobility was analyzed from shifts in both T_g and modulus behavior.

3.5. Mechanical characterization

Mechanical testing, including tensile, flexural, and impact tests, was conducted to evaluate the effects of ECO on the properties of PLA. All tests were performed on five replicates for each formulation to ensure reliability and account for variability. Tensile testing was carried out using a universal testing machine (Instron 3382, Massachusetts, USA), equipped with a 5kN load cell, following the ASTM D638 standard.[34] The tests were conducted at a crosshead speed of 5 mm min^{-1} using dog-bone-shaped specimens to measure the tensile strength, elongation at break, and modulus. Flexural tests were performed according to the ASTM D790 standard,[35] using the same testing machine under identical environmental conditions. Impact tests were conducted on notched Izod specimens using an impact tester (Zwick/Roell HIT25P, Ulm, Germany) in compliance with the ASTM D256 standard.[36] A 2.75 J capacity pendulum hammer was used for all tests. All tests were performed on five replicates, and the reported values represent the average results.

3.6. Morphological analysis

The tensile and impact-fractured surfaces of PLA and ECO–PLA samples were analyzed using scanning electron microscopy (SEM) (Phenom-World, BV, North Brabant) to examine their morphological characteristics. A thin gold coating was applied to the surfaces to improve conductivity, and the analysis was performed at an operating voltage of 10 kV.

4. Results and discussion

Camelina oil, known for its high unsaturated content, was epoxidized using hydrogen peroxide and formic acid, with Amberlite ion exchange resin (H^+) serving as the catalyst. The resulting epoxidized oil was then employed as a plasticizer for PLA. Various proportions of ECO (5%, 10%, and 15%) were blended with PLA through injection molding to develop the desired blends. Furthermore, the characterization of the synthesized ECO and the evaluation of the developed blends for their thermal and chemical properties are discussed in the subsequent sections. Scheme 1 illustrates the epoxidation process of camelina oil, and Scheme 2 depicts the proposed chemical interactions between ECO and PLA, potentially involving hydrogen bonding and esterification/transesterification.

4.1. FTIR analysis

FTIR spectroscopy provided essential insights into the molecular interactions between ECO and PLA, confirming both the

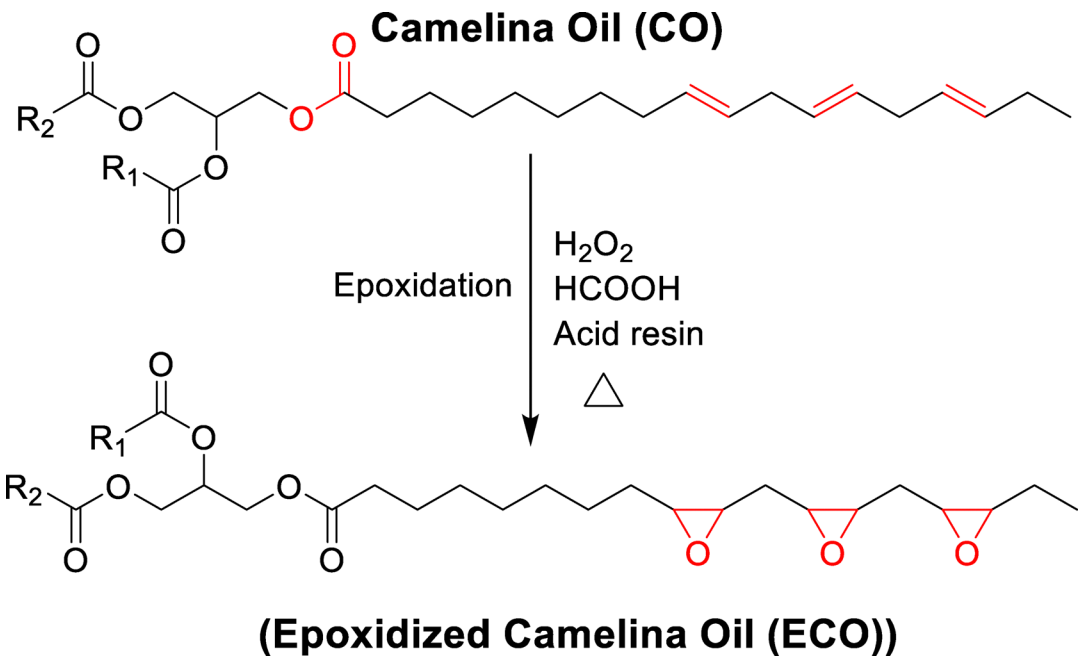

Scheme 1 Epoxidation of camelina oil in the presence of acidic ion exchange resin.

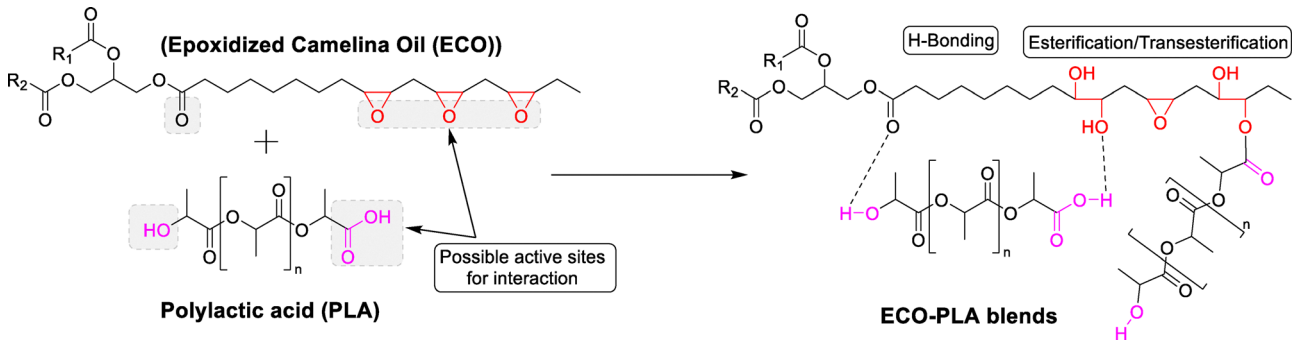

Scheme 2 Proposed chemical interactions of ECO with PLA *via* hydrogen bonding and or esterification/transesterification.

successful epoxidation of camelina oil and the plasticizing effect of ECO in the blends. For the pure ECO sample, the epoxidation was confirmed by the disappearance of the C═C–H stretching peak at around 3014 cm^{-1}, characteristic of camelina oil's unsaturated double bonds as can be seen in Fig. 1(a). This was replaced by a new peak at approximately 825 cm^{-1}, associated with the symmetric and asymmetric stretching of the oxirane (epoxide) ring, indicating successful conversion of double bonds to reactive epoxide groups.[37,38] These epoxide groups are important for compatibility with PLA, as they facilitate intermolecular interactions and potential chemical reactions with PLA functional groups. In the ECO–PLA blends (Fig. 1(b)), several notable changes in the FTIR spectrum further highlighted the interactions between ECO and PLA. The carbonyl (C═O) stretching peak of PLA, typically observed at around 1750 cm^{-1}, shifted slightly to lower wavenumbers in the ECO–PLA blends, especially at higher ECO contents (10% and 15%). This shift suggests that hydrogen bonding occurs between PLA's carbonyl groups and hydroxyl groups formed from the epoxide ring opening in ECO, which reduces the vibrational energy and shifts the absorption frequency of the carbonyl group.[39,40] A broad band appeared in the 3500–3200 cm^{-1} region, which corresponds to O–H stretching vibrations, indicating the presence of hydroxyl groups formed as a result of epoxide ring opening in ECO.[41] The presence of these hydroxyl groups, likely forming hydrogen bonds with PLA, confirms the strong interaction between ECO and PLA.[42] These interactions contribute to the plasticizing effect observed in the blends, where the increased mobility of PLA chains results in improved flexibility and toughness.

Additionally, the FTIR spectrum showed changes in the aliphatic C–H stretching region (2950–2850 cm^{-1}) as the ECO content increased, reflecting the introduction of more aliphatic chains from ECO. While the intensity of these peaks did not significantly increase, their presence confirms the successful

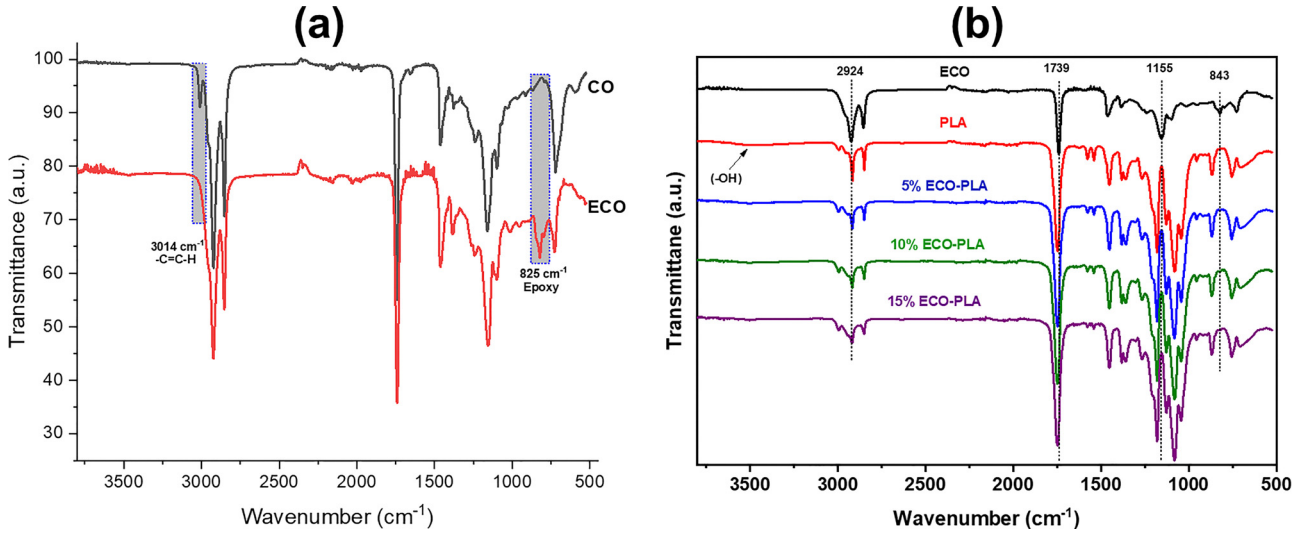

Fig. 1 ATR-FTIR spectra of (a) CO and ECO and (b) neat PLA, 5% ECO–PLA, 10% ECO–PLA, and 15% ECO–PLA.

integration of ECO, which contributes to improved ductility and reduced stiffness in the blends.[43]

4.2. NMR analysis

Fig. 2 highlights the ^{1}H NMR spectra of camelina oil (CO) before and after epoxidation, illustrating the successful transformation of unsaturated double bonds into oxirane (epoxide) groups. In the spectrum of unmodified CO, prominent peaks were observed at 5.3–5.5 ppm, corresponding to the protons of olefinic double bonds (–HC═CH–). The disappearance of peaks associated with double bonds in the ECO spectrum indicates their successful conversion into oxirane groups. Simultaneously, the peaks appearance in the range of 2.8–3.2 ppm corresponds to protons in the oxirane rings, confirming the formation of epoxide groups. This spectral shift is a definitive indicator of the successful epoxidation process.[37] In the aliphatic region, signals in the range of 0.8–2.5 ppm correspond to the methylene (–CH_2–) and methyl (–CH_3) groups of the fatty acid chains.[44] These peaks are present in both spectra, indicating that the hydrocarbon backbone remains intact during the epoxidation process. While their intensities remain largely unchanged, the slight differences in peak shape suggest minor structural rearrangements in the chains caused by the introduction of epoxide groups. The glycerol backbone protons (–CH_2–O–) are observed in the region of 4.1–4.3 ppm in the CO spectrum.[45] In the ECO spectrum, these peaks appear shifted and slightly less intense, likely due to changes in the electronic environment caused by the epoxidation. Additionally, a broad peak emerges at around 3.3–3.5 ppm in the ECO spectrum, corresponding to hydroxyl protons formed due to partial ring-opening reactions of the epoxide groups. These hydroxyl groups enhance hydrogen bonding with the carbonyl groups of PLA, improving the miscibility and interfacial interactions in ECO–PLA blends.

Furthermore, the absence of peaks in the 5.3–5.5 ppm region of the ECO spectrum indicates that the olefinic double

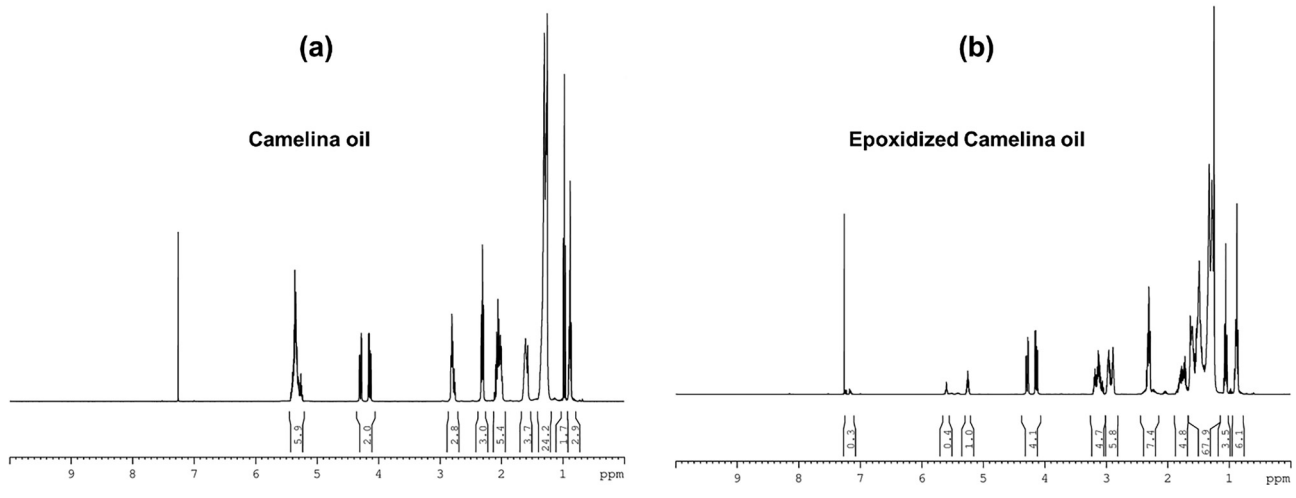

Fig. 2 ^{1}H NMR spectra of (a) CO and (b) ECO.

bonds were largely consumed during epoxidation, consistent with the 92.6% conversion calculated from ^{1}H NMR integration. Based on this conversion, approximately 5.1 mmol of epoxide groups per gram of sample were obtained.[46] Similarly, in another study, the epoxidation percentage was determined to be 94.5%, based on the vinyl signals observed between 5.3 and 5.5 ppm in the ^{1}H NMR spectrum.[47] The significant reduction of these peaks in the ECO spectrum indicates that most of the double bonds have been successfully converted to epoxide groups. The absence of residual olefinic protons and the presence of strong oxirane proton peaks indicate a high degree of epoxidation, crucial for the enhanced plasticizing efficiency of ECO. The density of oxirane groups facilitates intermolecular interactions with PLA, including hydrogen bonding and esterification reactions, which improve the ductility and toughness of PLA, as previously discussed by Chieng *et al.*[41] and Thuy *et al.*[48]

The FTIR and NMR results not only confirm the formation of oxirane rings in the epoxidized camelina oil but also provide evidence for chemical interactions between the epoxidized oil and PLA chains. The downward shift of the PLA carbonyl absorption band and the appearance of a broad hydroxyl region indicate the presence of hydrogen bonding between the hydroxyl groups formed during partial ring opening of the epoxy groups and the carbonyl oxygen atoms of PLA. Hydrogen bonding increases temporary physical cross links that restrict local chain packing but simultaneously increase segmental mobility by weakening the strong intermolecular interactions that normally lead to brittle fracture in neat PLA. Several studies report that hydrogen bonded plasticizers reduce the glass transition temperature of PLA by increasing the free volume and promoting cooperative chain motion, which directly enhances ductility and impact resistance. In addition to hydrogen bonding, the residual epoxy groups in ECO may undergo limited ester exchange reactions with the terminal hydroxyl groups of PLA during melt blending. Such reactions create weakly bonded junction points that improve compatibility and reduce phase separation. These chemical interactions collectively explain the significant increase in elongation at break and the transition from brittle to ductile fracture behavior observed in the SEM images. Prior literature on epoxidized plant oils in PLA systems also shows that strong secondary interactions and partial ester linkages increase chain mobility and substantially improve toughness, which is consistent with the mechanical performance trends observed in this study.

4.3. Thermal analysis

As shown in Fig. 3 and Table 1, the DSC thermograms include both the cooling scan and the second heating scan to illustrate the influence of ECO on the thermal behavior of PLA. The analysis indicated a progressive reduction in the T_g of PLA as the ECO content was increased from 5% to 15%. Neat PLA typically has a T_g of around 60 °C, a temperature at which the polymer transitions to a more flexible, rubbery state from a rigid, glassy state. The 5% ECO–PLA blend showed a T_g decrease to approximately 55.46 °C, while the 10% and 15% ECO–PLA blends reduced the T_g further to around 53.86 °C and 53.62 °C, respectively. Similarly, the cold crystallization temperature of pure PLA was reduced from 95.4 °C to 91.2 °C upon incorporation of 5% ECO, while no significant differences were observed in 10% and 15% ECO–PLA blends. This downward shift in T_g and cold crystallization temperature is indicative of the plasticizing effect of ECO, which enhances the polymer chain mobility.[41,49] Increased chain mobility implies that the polymer can absorb more stress without fracturing, thereby reducing brittleness and enabling improved flexibility.[42] The melting temperature (T_m) showed a slight reduction from neat PLA's typical melting point, suggesting that the crystalline regions within PLA were somewhat disrupted by the inclusion of ECO.[50]

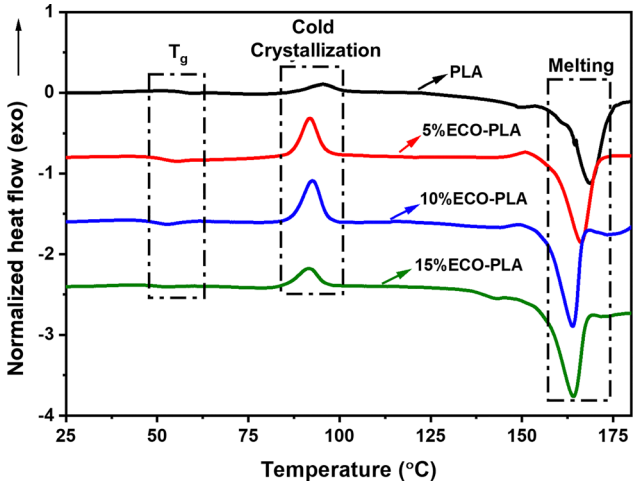

Fig. 3 DSC thermograms of neat PLA and its blends containing 5%, 10%, and 15% ECO.

Table 1 Glass transition temperature (T_g), onset temperature (T_{onset}), degradation temperature ($T_{degradation}$), and temperature at 5% weight loss ($T_{5\%}$) for PLA and ECO-based blends

Sample	T_g	T_{onset}	$T_{degradation}$	$T_{5\%}$
PLA	59.41	341.83	366.22	322.80
5%ECO–PLA	55.46	338.72	364.81	321.19
10%ECO–PLA	53.86	337.22	364.96	322.67
15%ECO–PLA	53.62	332.21	362.54	312.59

The TGA curve (Fig. 4) provides valuable insights into the thermal stability and decomposition behavior of neat PLA and ECO–PLA blends with varying ECO content (5%, 10%, and 15%). In the TGA plot, the neat PLA sample (black line) begins to decompose at a higher onset temperature, underscoring its improved thermal stability in contrast to the ECO–PLA blends. As the ECO content increases, the onset of decomposition shifts slightly to lower temperatures, particularly for the 10% and 15% ECO–PLA blends, as can be seen in Table 1. This shift indicates that the addition of ECO reduces the thermal stability of PLA, likely due to the lower decomposition temperature of ECO and the plasticizing effect. The plasticizer weakens intermolecular forces within the PLA matrix, increases chain mobility, and introduces more thermally labile components, contributing to earlier thermal degradation.[51]

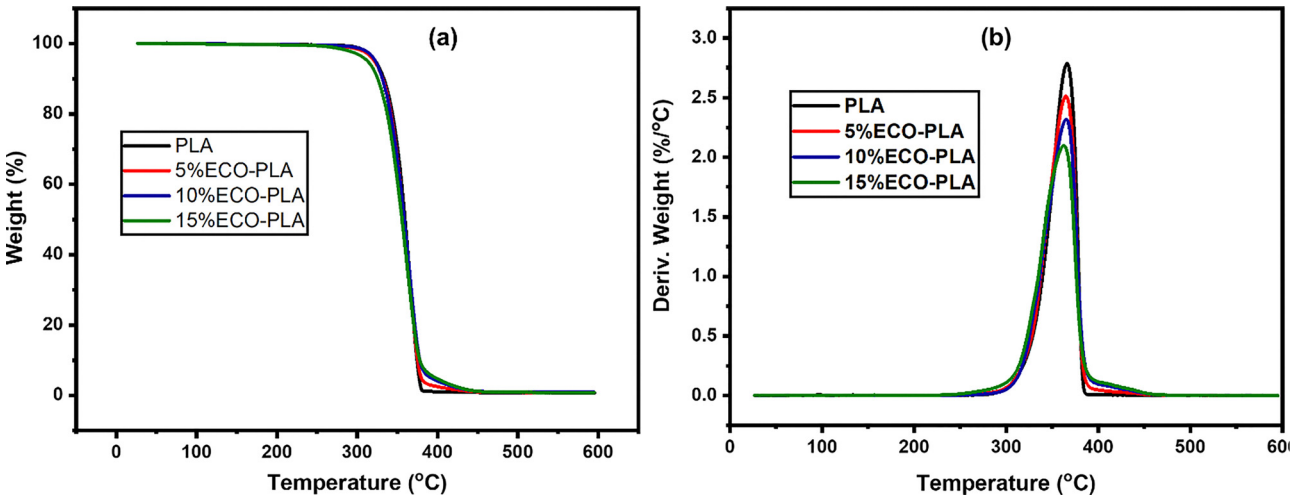

Fig. 4 TGA (a) and DTGA (b) curves of neat PLA and PLA–ECO blends (5% ECO–PLA, 10% ECO–PLA, and 15% ECO–PLA).

All samples exhibit a sharp weight loss around 300 °C–350 °C, corresponding to the primary decomposition phase of PLA, where rapid depolymerization occurs. This phase results in significant weight loss, primarily due to the breakdown of the polymer backbone into volatile products. While the degradation behavior is consistent across all blends, the weight loss in this region is slightly more pronounced for the 15% ECO–PLA blend, as indicated by its notably lower $T_{5\%}$ value compared to neat PLA (Table 1). This trend suggests that the increase in content of ECO accelerates thermal decomposition, a behavior commonly observed in plasticized polymer systems. Plasticizers, having lower thermal stability and increasing the free volume within the polymer matrix, facilitate earlier chain scission and enhance the rate of decomposition.[52,53] At higher temperatures, the TGA curves level off, indicating the completion of the decomposition process. Minimal residual weight remains for both neat PLA and ECO–PLA blends, signifying almost complete thermal breakdown. This behavior confirms that while the incorporation of ECO slightly decreases the thermal stability of PLA, the blends still exhibit thermal stability adequate for most processing and application conditions.

4.4. Dynamic mechanical properties

Dynamic mechanical snalysis (DMA) was used to evaluate the viscoelastic behavior of ECO–PLA blends across a temperature range, focusing on how ECO influences the storage modulus (E'), loss modulus (E''), and tan δ. These parameters help to understand the elastic and viscous responses of the material, as well as its energy dissipation characteristics, providing insights into the flexibility and damping capacity of the blends. Fig. 5(a) shows the elastic behavior of the material as it deforms under an oscillating force. The storage modulus is high in the glassy region, indicating that the material is rigid. As the temperature increases, E' decreases, showing the material's transition from a glassy to a rubbery state. Beyond this region, the storage modulus began to rise again due to cold crystallization of PLA within the blends. The onset of cold crystallization shifted to a lower temperature with increasing ECO content, suggesting that ECO acted as a plasticizing component that enhanced chain mobility and promoted earlier crystallite formation.[54,55] Fig. 5(b) shows the viscous behavior of the material, representing the amount of energy lost as heat during deformation. A peak in the loss modulus usually corresponds to the T_g, where the material's damping properties are highest. The addition of ECO has affected the height and position of this peak, indicating changes in the T_g and the damping characteristics of the blend. A peak in the tan δ curve (Fig. 5(c)) is another indicator of the T_g. Materials with a higher tan δ at room temperature can be better at absorbing and dissipating energy, such as in impact-resistant applications. At low ECO content, the tan δ peak increases, suggesting enhanced energy dissipation capability. However, at higher ECO loadings, the peak height slightly decreases, indicating that excessive plasticization may reduce damping efficiency.

4.5. Mechanical properties

Fig. 6(a) presents the stress–strain behavior of neat PLA and PLA–ECO blends with 5%, 10%, and 15% ECO. The stress–strain behavior demonstrates how the material deforms under tensile force, with the slope of the initial linear section indicating stiffness and the area under the curve representing toughness. For pure PLA (0% ECO), the steep initial slope reflects high stiffness and rigidity, but the curve terminates abruptly at maximum stress, indicating brittle failure with minimal deformation. In contrast, as ECO content increases, the curves become less steep and extend further along the strain axis, reflecting reduced stiffness and enhanced ductility. This behavior aligns with lubricity theory, which explains that ECO acts as a lubricant, reducing internal friction and allowing polymer chains to slide past one another more freely. As a result, blends with higher ECO content exhibit greater chain mobility, enabling them to stretch significantly further before failure.[56] The increase in elongation at break, as observed in Fig. 6(b),

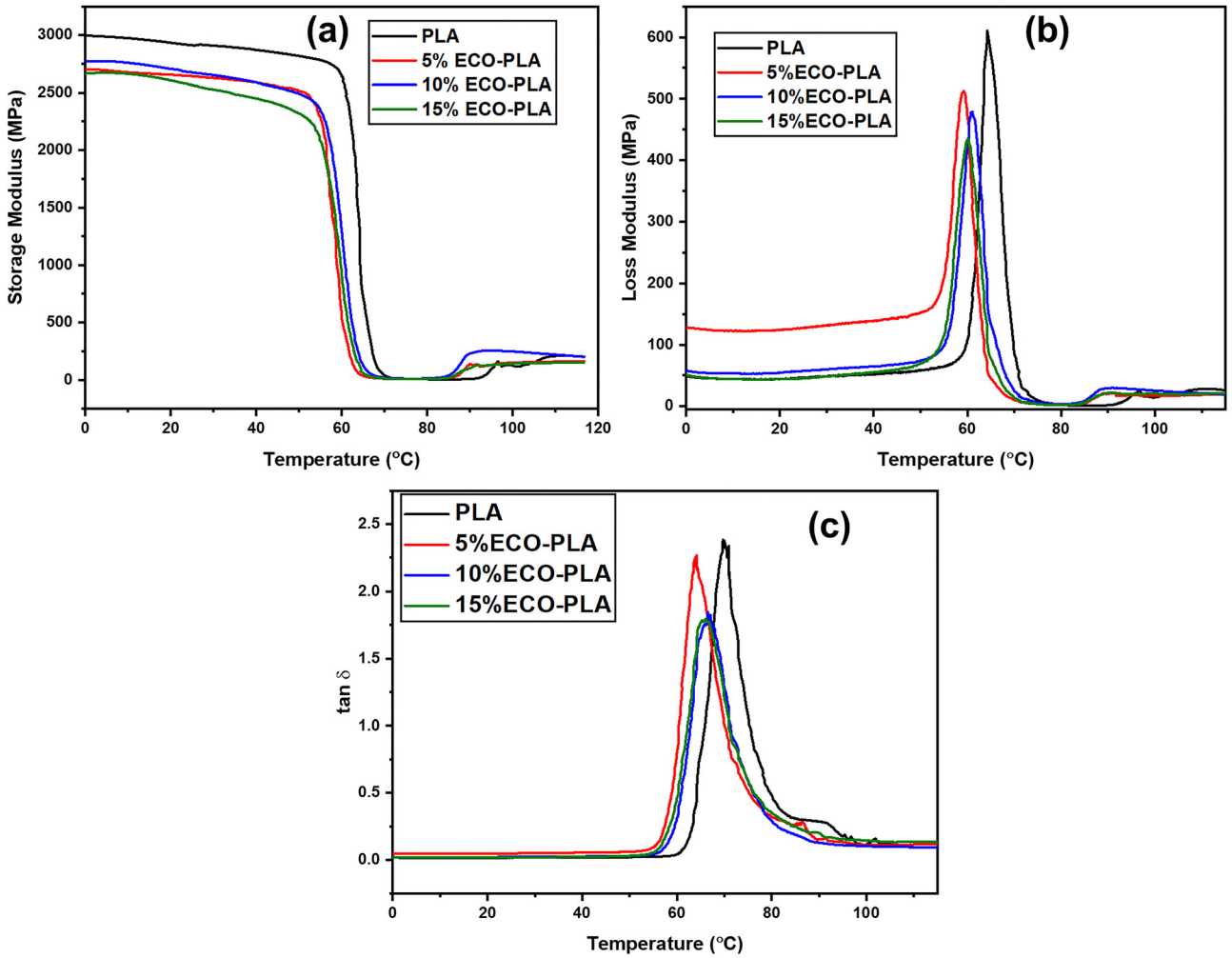

Fig. 5 DMA curves of PLA and its blends containing 5%, 10%, and 15% ECO. (a) storage modulus, (b) loss modulus and (c) tan δ.

further supports the gel theory, which states that plasticizers like ECO disrupt and replace strong polymer–polymer interactions (such as hydrogen bonds and van der Waals forces) with weaker plasticizer–polymer interactions.[41] This disruption reduces the gel-like structure of the polymer matrix, increasing flexibility and extensibility. This mechanism has been widely reported in the literature,[41,57,58] where the addition of epoxidized oils to PLA has been shown to increase elongation at break significantly, transitioning PLA from a brittle to a more ductile one.

The tensile and flexural moduli, as shown in Fig. 6(c), decrease with increasing ECO content, reflecting a reduction in stiffness. This behavior is explained by the gel theory, as the plasticizer disrupts the dense packing of polymer chains, increasing free volume and chain mobility. This reduction in intermolecular interactions weakens the polymer network, making the material less resistant to deformation under tensile and bending loads.

As shown in Fig. 6(b), the tensile strength, which represents the maximum stress a material can endure before failure, decreases with higher ECO contents. This is due to the reduction in intermolecular forces within the polymer matrix, which lowers its load-bearing capacity. However, the elongation at break increases dramatically, indicating that the material can deform to a much greater extent before failure. This trade-off between elongation at break and tensile strength is a well-documented characteristic of plasticized polymers. Al-Mulla *et al.*[20] found that adding epoxidized palm oil to a PLA/polycaprolactone (PCL) blend decreased tensile strength while markedly increasing elongation at break, indicating improved flexibility.

Fig. 6(d) presents the notched impact strength of PLA–ECO blends, which quantifies the material's ability to absorb and dissipate energy during sudden impact loading. Pure PLA exhibits relatively low impact strength due to its brittle nature. However, as the ECO content increases, impact strength improves significantly. This improvement can be attributed to the ECO's toughening effect, which enhances energy dissipation by increasing chain mobility and reducing stress concentrations at the point of impact. The enhanced impact resistance is consistent with lubricity theory, as the plasticizer reduces friction between polymer chains, allowing for better energy

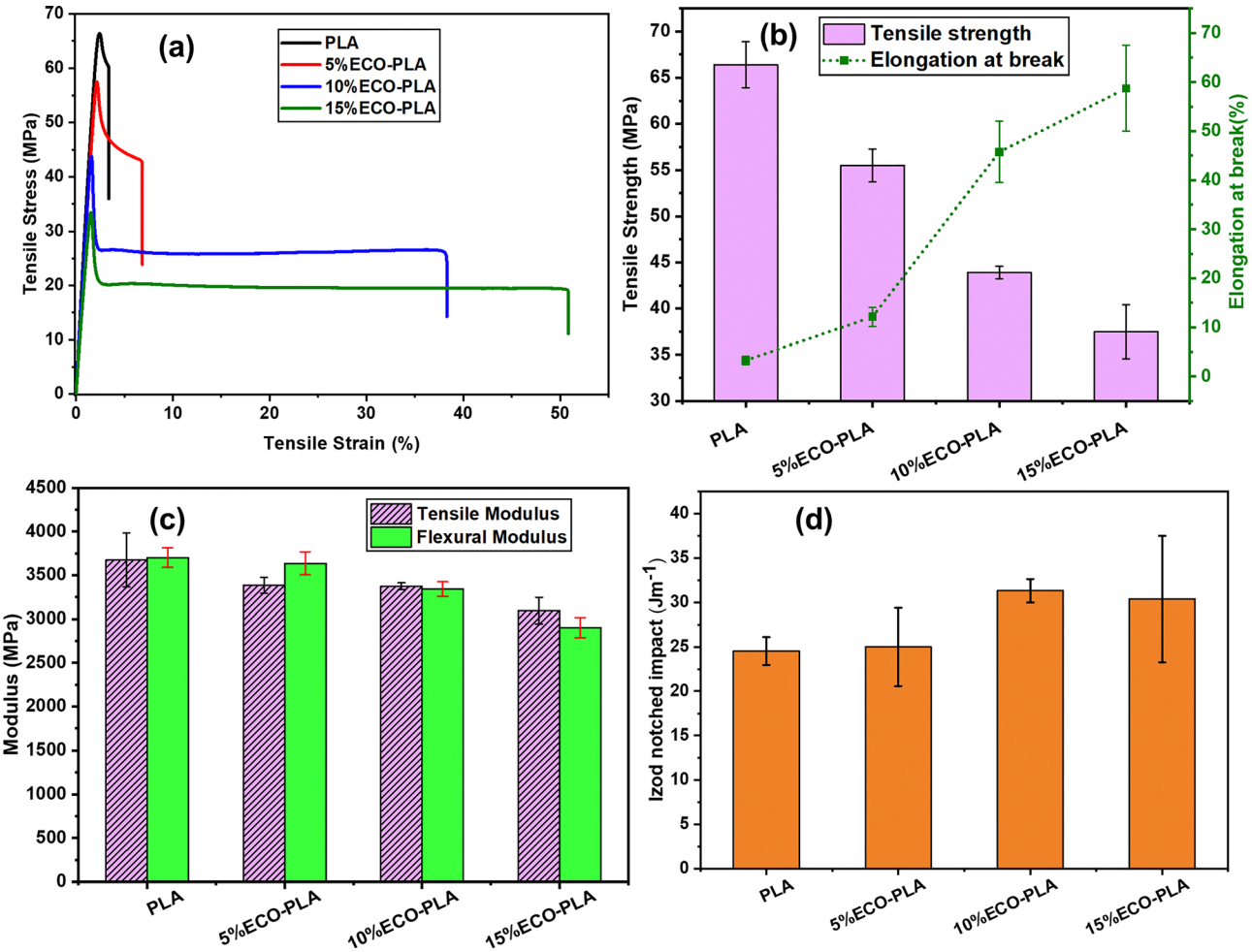

Fig. 6 (a) Stress–strain curves, (b) and (c) tensile properties, and (d) Izod notched impact strength of PLA and its blends containing 5%, 10%, and 15% ECO.

redistribution during deformation. Several studies have demonstrated this effect. Orue *et al.*[59] confirmed that epoxidized linseed and soybean oils increased the impact strength of PLA composites, supporting the toughening mechanism through improved polymer chain mobility. Their findings further prove that the addition of ECO enhances ductility and stress dissipation. Additionally, Tee *et al.*[60] demonstrated that epoxidized palm oil and soybean oil improved PLA's toughness, effectively reducing stress concentrations and promoting better energy dissipation.

While the overall trends show that ECO enhances ductility and impact resistance, the mechanical response of the 15% ECO blend suggests the onset of over plasticization. The substantial drop in tensile strength and modulus, combined with the extremely large elongation at break, indicates that the PLA matrix may approach saturation at this concentration. When saturation occurs, the polymer loses cohesive strength and deformation becomes dominated by viscous flow rather than controlled plastic deformation.

SEM analysis supports this interpretation. The fracture surface of the 15% blend shows large deformation zones, extensive fibrillation, and broad voids, all of which reveal very high chain mobility and reduced structural integrity. In contrast, the 10% blend shows a more uniform ductile morphology with finer energy absorbing structures, indicating a more balanced plasticization effect. The DMA results provide further confirmation. The storage modulus of the 15% ECO blend decreases more sharply across the temperature range compared to the 5% and 10% blends, and the glass transition temperature shifts to lower values. These observations indicate a highly softened matrix and reduced intermolecular cohesion, characteristic of over plasticized systems.

This behavior is consistent with findings from related studies on epoxidized plant oils in PLA systems. Prior work has shown that, at high plasticizer concentrations, micro scale heterogeneity and partial phase separation may occur, leading to weaker load bearing capability even though ductility improves.[61–63] These comparisons suggest that the 10% ECO blend offers the best balance of strength, toughness, and flexibility, while the 15% blend approaches the upper compatibility limit for ECO in PLA.

4.6. Morphological analysis

The SEM micrographs of tensile fractured surfaces for neat PLA, 5%ECO–PLA, 10%ECO–PLA, and 15%ECO–PLA as shown

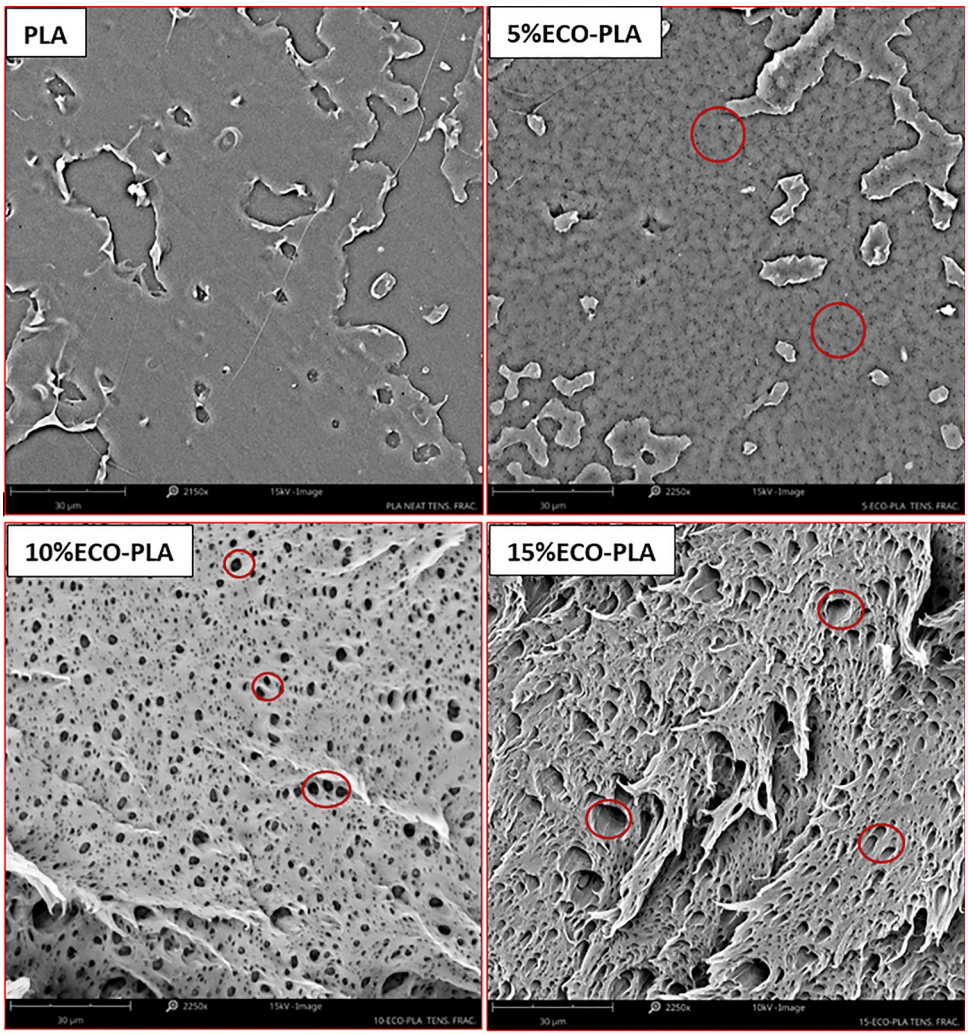

Fig. 7 SEM micrographs of tensile fractured surfaces for neat PLA, 5%ECO–PLA, 10%ECO–PLA, and 15%ECO–PLA.

in Fig. 7 demonstrate the progressive impact of ECO on the fracture morphology of PLA. Neat PLA exhibits a smooth and relatively featureless fracture surface, characteristic of brittle failure. This is indicative of a rigid material with strong intermolecular interactions and limited energy dissipation, consistent with its high tensile modulus and low elongation at break.[64] In contrast, the addition of 5% ECO introduces a rougher fracture surface with small voids and localized plastic deformation. These features suggest the onset of ductility as ECO begins to disrupt the rigid PLA matrix, reducing friction between polymer chains and enabling limited chain mobility. At 10% ECO, the fracture surface shows significant roughness with pronounced voids and fibrillar structures, indicative of increased cavitation and polymer chain stretching during deformation. This reflects a transition to ductile failure, supported by the substantial increase in elongation at break observed in the mechanical tests. The addition of 15% ECO further accentuates this trend, with extensive fibrillation and a highly rough fracture surface, characteristic of highly ductile behavior. The presence of large voids and stretched fibrils highlights enhanced chain mobility and energy dissipation, although excessive plasticization at this level may reduce tensile strength due to a less cohesive polymer matrix. These observations align with the lubricity and gel theories, which describe how ECO disrupts polymer–polymer interactions, facilitates chain mobility, and transitions the material from brittle to ductile behavior.[41,56]

The SEM micrographs of the impact-fractured surfaces, as displayed in Fig. 8, highlight the gradual influence of ECO on the fracture behavior and mechanisms of PLA. The fracture surface of neat PLA is smooth, with sharp-edged cracks indicative of brittle failure, where rapid crack propagation occurs with minimal energy absorption. This morphology reflects the inherent rigidity and brittleness of PLA, consistent with its low impact strength.[65] With the incorporation of 5% ECO, the fracture surface becomes rougher, with small deformation zones and less pronounced crack propagation, suggesting the onset of ductile behavior. ECO acts as a plasticizer, disrupting the rigid PLA structure and enabling localized chain mobility, resulting in improved energy absorption during impact. At 10%

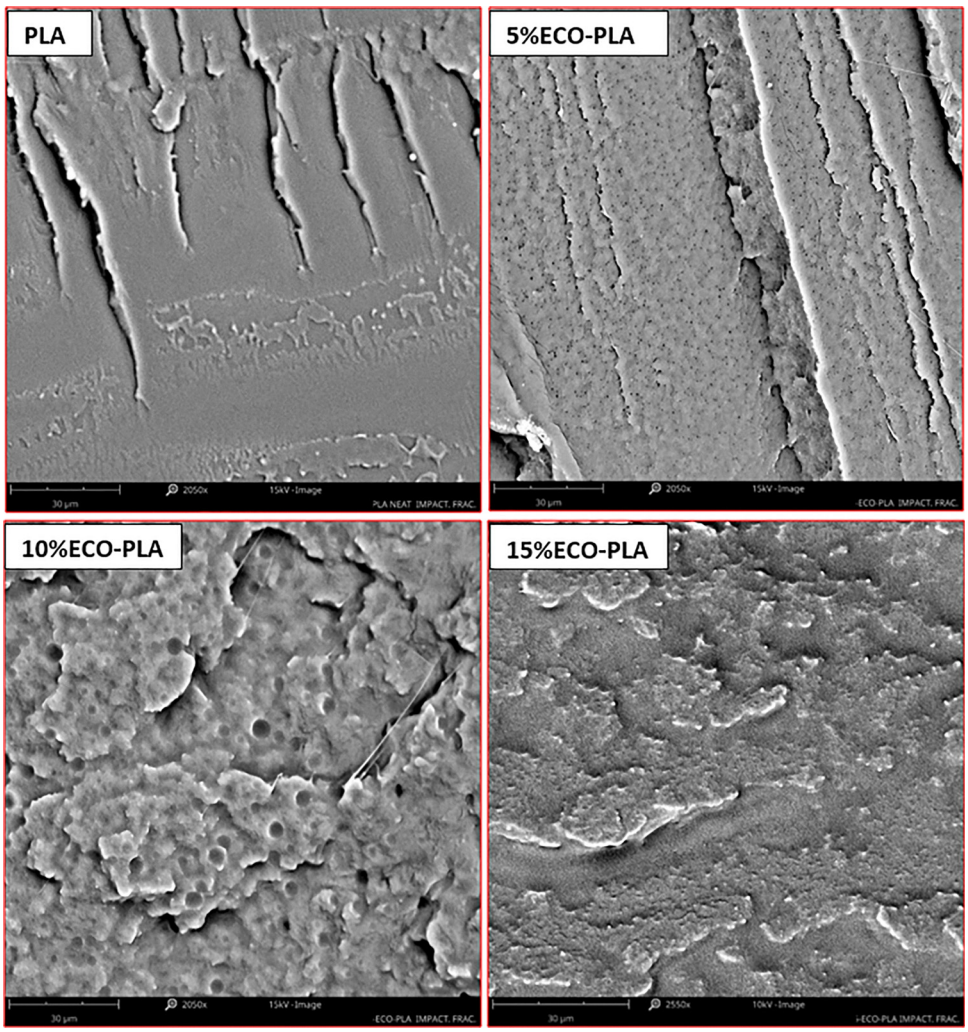

Fig. 8 SEM micrographs of impact fractured surfaces for neat PLA, 5% ECO–PLA, 10% ECO–PLA, and 15% ECO–PLA.

ECO content, the fracture surface exhibits significant roughness, with visible voids, micro-tears, and substantial plastic deformation. These features indicate a clear transition to ductile fracture, where the material effectively dissipates stress and delays crack propagation. The enhanced toughness at this ECO level aligns with the lubricity theory, which posits that ECO reduces friction between polymer chains, and the gel theory, which explains that ECO disrupts strong polymer–polymer interactions, increasing flexibility.[53]

At 15% ECO, the fracture surface becomes highly rough and dominated by extensive deformation zones, voids, and fibrillation, indicating maximum energy dissipation and ductile behavior. The increased roughness and deformation zones compared to a lower ECO content suggest that the material absorbs significant impact energy before failure, although the excessive matrix disruption at this high ECO content may lead to reduced tensile strength. This behavior is consistent with the findings in the literature, where the increasing plasticizer content enhances ductility and toughness but may compromise the cohesive strength of the polymer matrix.[66,67]

5. Conclusions

Camelina oil with high unsaturated contents (90%) was epoxidized by reacting it with hydrogen peroxide and formic acid in the presence of Amberlite ion exchange resin (H^+) as a catalyst to facilitate the reaction. NMR spectroscopy validated the epoxidation process by showing the absence of olefinic proton peaks at 5.3–5.5 ppm and the emergence of oxirane proton peaks in the range of 2.8–3.2 ppm, confirming a high degree of functionalization. FTIR spectroscopy further validated the chemical modification with the disappearance of –C=C–H stretching vibrations and the emergence of characteristic oxirane peaks at around 825 cm^{-1}. FTIR also revealed shifts in the carbonyl stretching region of PLA, confirming hydrogen bonding and improved compatibility between ECO and PLA. The ECO was blended with PLA at various ratios (5%, 10%, and 15%) and evaluated for its mechanical, thermal, and morphological properties. The inclusion of ECO significantly enhanced the elongation at break (up to 1680%) and impact strength (up to 25%) of PLA, transitioning it from brittle to ductile behavior. SEM analysis revealed progressive changes in fracture

morphology, demonstrating enhanced flexibility and toughness. Thermal analysis indicated a reduction in the T_g, validating the plasticizing effect of ECO and its role in increasing polymer chain mobility.

The combined insights from NMR and FTIR highlight the successful chemical transformation and compatibility of ECO with PLA, attributed to the oxirane and hydroxyl groups facilitating strong intermolecular interactions. These findings underscore the potential of ECO as a renewable and effective alternative to petroleum-based plasticizers, enhancing the performance of PLA for applications in packaging, biomedical materials, and other sectors requiring flexibility and toughness.

Author contributions

M. A.: investigation, methodology, data curation, formal analysis, visualization, writing – original draft, and writing – review and editing. M. H.: investigation, methodology, data curation, formal analysis, writing – original draft preparation, and writing – review and editing. A. R.: investigation, methodology, data curation, formal analysis, writing – original draft preparation, and writing – review and editing. A. K. M.: conceptualization, investigation, methodology, validation, supervision, resources, funding acquisition, and writing – review and editing. M. M.: conceptualization, investigation, methodology, validation, supervision, resources, funding acquisition, and writing – review and editing. All authors contributed to the discussion, reviews and approval of the manuscript for publication.

Conflicts of interest

The authors declare that they have no known competing financial interests or personal relationships that could have appeared to influence the work reported in this paper.

Data availability

The datasets supporting the findings of this study are available from the corresponding author upon reasonable request. All data generated or analyzed during this study, including raw experimental results, characterization files (*e.g.*, FTIR, TGA, DSC, and NMR) and mechanical testing data have been archived and can be shared in compliance with journal policy. No publicly archived datasets were used in this research.

Acknowledgements

This study was financially supported by the Ontario Ministry of Agriculture, Food and Rural Affairs (OMAFRA) – University of Guelph, the Bioeconomy Industrial Uses Research Program Theme (Project No. 030706), the OMAFRA – Ontario Agri-Food Research Initiative (Project No. 056442), the Natural Sciences and Engineering Research Council of Canada (NSERC), Discovery Grants Program (Project No. 401716) and the NSERC Canada Research Chair (CRC) Program Project No. 460788.

References

1 H. Miyagawa, A. K. Mohanty, M. Misra and L. T. Drzal, Thermo-physical and impact properties of epoxy containing epoxidized linseed oil, 1: Anhydride-cured epoxy, *Macromol. Mater. Eng.*, 2004, **289**, 629–635, DOI: 10.1002/MAME.200400004.
2 H. Miyagawa, M. Misra, L. T. Drzal and A. K. Mohanty, Fracture toughness and impact strength of anhydride-cured biobased epoxy, *Polym. Eng. Sci.*, 2005, **45**, 487–495, DOI: 10.1002/pen.20290.
3 J. Qin, M. Woloctt and J. Zhang, Use of polycarboxylic acid derived from partially depolymerized lignin as a curing agent for epoxy application, *ACS Sustainable Chem. Eng.*, 2014, **2**, 188–193, DOI: 10.1021/sc400227v.
4 ASTM. ASTM D6400-21, Standard Specification for Labeling of Plastics Designed to be Aerobically Composted in Municipal or Industrial Facilities 2022:3, DOI: 10.1520/D6400-23.
5 R. Bhardwaj and A. K. Mohanty, Advances in the Properties of Polylactides Based Materials: A Review, *J. Biobased Mater. Bioenergy*, 2008, **1**, 191–209, DOI: 10.1166/jbmb.2007.023.
6 N. Wu, H. Zhang and G. Fu, Super-tough Poly(lactide) Thermoplastic Vulcanizates Based on Modified Natural Rubber, *ACS Sustainable Chem. Eng.*, 2017, **5**(1), 78–84, DOI: 10.1021/acssuschemeng.6b02197.
7 D. Garlotta, A Literature Review of Poly(Lactic Acid), *J. Polym. Environ.*, 2001, **9**, 63–84, DOI: 10.1023/A:1020200822435.
8 W. Ren, X. Pan, G. Wang, W. Cheng and Y. Liu, Dodecylated lignin-: G -PLA for effective toughening of PLA, *Green Chem.*, 2016, **18**, 5008–5014, DOI: 10.1039/c6gc01341d.
9 S. C. Mauck, S. Wang, W. Ding, B. J. Rohde, C. K. Fortune and G. Yang, *et al.*, Biorenewable Tough Blends of Polylactide and Acrylated Epoxidized Soybean Oil Compatibilized by a Polylactide Star Polymer, *Macromolecules*, 2016, **49**, 1605–1615, DOI: 10.1021/acs.macromol.5b02613.
10 X. Zhao, H. Hu, X. Wang, X. Yu, W. Zhou and S. Peng, Super tough poly(lactic acid) blends: A comprehensive review, *RSC Adv.*, 2020, **10**, 13316–13368, DOI: 10.1039/d0ra01801e.
11 H. Liu and J. Zhang, Research progress in toughening modification of poly(lactic acid), *J. Polym. Sci., Part B: Polym. Phys.*, 2011, **49**, 1051–1083, DOI: 10.1002/polb.22283.
12 M. Murariu, Y. Paint, O. Murariu, F. Laoutid and P. Dubois, Tailoring and Long-Term Preservation of the Properties of PLA Composites with ''Green'' Plasticizers, *Polymers*, 2022, **14**(22), 4836, DOI: 10.3390/polym14224836.
13 T. Tábi, T. Ageyeva and J. G. Kovács, Improving the ductility and heat deflection temperature of injection molded Poly(lactic acid) products: A comprehensive review, *Polym. Test.*, 2021, 101, DOI: 10.1016/j.polymertesting.2021.107282.
14 S. Sun, Y. Weng and C. Zhang, Recent advancements in bio-based plasticizers for polylactic acid (PLA): A review, *Polym. Test.*, 2024, **140**, 108603, DOI: 10.1016/j.polymertesting.2024.108603.
15 G. Kfoury, J. M. Raquez, F. Hassouna, J. Odent, V. Toniazzo and D. Ruch, *et al.*, Recent advances in high performance poly(lactide): From ''green'' plasticization to super-tough

materials via (reactive) compounding, *Front. Chem.*, 2013, **1**, 1–46, DOI: 10.3389/fchem.2013.00032.

16 S. Sun, Y. Weng, Y. Han and C. Zhang, Plasticization mechanism of biobased plasticizers comprising polyethylene glycol diglycidyl ether-butyl citrate with both long and short chains on poly(lactic acid), *Int. J. Biol. Macromol.*, 2024, **276**, 133948, DOI: 10.1016/j.ijbiomac.2024.133948.

17 O. Valerio, J. M. Pin, M. Misra and A. K. Mohanty, Synthesis of glycerol-based biopolyesters as toughness enhancers for polylactic acid bioplastic through reactive extrusion, *ACS Omega*, 2016, **1**, 1284–1295, DOI: 10.1021/acsomega.6b00325.

18 Y. Xia and R. C. Larock, Vegetable oil-based polymeric materials: Synthesis, properties, and applications, *Green Chem.*, 2010, **12**, 1893–1909, DOI: 10.1039/c0gc00264j.

19 G. Mehta, A. K. Mohanty, M. Misra and L. T. Drzal, Biobased resin as a toughening agent for biocomposites, *Green Chem.*, 2004, **6**, 254–258, DOI: 10.1039/b316658a.

20 E. A. J. Al-Mulla, W. M. Z. W. Yunus, N. A. B. Ibrahim and M. Z. A. Rahman, Properties of epoxidized palm oil plasticized polytlactic acid, *J. Mater. Sci.*, 2010, **45**, 1942–1946, DOI: 10.1007/s10853-009-4185-1.

21 L. Quiles-Carrillo, S. Duart, N. Montanes, S. Torres-Giner and R. Balart, Enhancement of the mechanical and thermal properties of injection-molded polylactide parts by the addition of acrylated epoxidized soybean oil, *Mater. Des.*, 2018, **140**, 54–63, DOI: 10.1016/j.matdes.2017.11.031.

22 O. Valerio, M. Misra and A. K. Mohanty, Poly(glycerol-co-diacids) Polyesters: From Glycerol Biorefinery to Sustainable Engineering Applications, A Review. ACS Sustain, *Chem. Eng.*, 2018, **6**, 5681–5693, DOI: 10.1021/acssuschemeng.7b04837.

23 G. Mashouf Roudsari, A. K. Mohanty and M. Misra, Study of the curing kinetics of epoxy resins with biobased hardener and epoxidized soybean oil, *ACS Sustainable Chem. Eng.*, 2014, **2**, 2111–2116, DOI: 10.1021/sc500176z.

24 A. Carbonell-Verdu, D. Garcia-Garcia, F. Dominici, L. Torre, L. Sanchez-Nacher and R. Balart, PLA films with improved flexibility properties by using maleinized cottonseed oil, *Eur. Polym. J.*, 2017, **91**, 248–259, DOI: 10.1016/j.eurpolymj.2017.04.013.

25 L. Quiles-Carrillo, M. M. Blanes-Martínez, N. Montanes, O. Fenollar, S. Torres-Giner and R. Balart, Reactive toughening of injection-molded polylactide pieces using maleinized hemp seed oil, *Eur. Polym. J.*, 2018, **98**, 402–410, DOI: 10.1016/j.eurpolymj.2017.11.039.

26 J. M. Ferri, D. Garcia-Garcia, L. Sánchez-Nacher, O. Fenollar and R. Balart, The effect of maleinized linseed oil (MLO) on mechanical performance of poly(lactic acid)-thermoplastic starch (PLA-TPS) blends, *Carbohydr. Polym.*, 2016, **147**, 60–68, DOI: 10.1016/j.carbpol.2016.03.082.

27 W. Liu, J. Qiu, M. E. Fei, R. Qiu and E. Sakai, Manufacturing of Thermally Remoldable Blends from Epoxidized Soybean Oil and Poly(lactic acid) via Dynamic Cross-Linking in a Twin-Screw Extruder, *Ind. Eng. Chem. Res.*, 2018, **57**, 7516–7524, DOI: 10.1021/acs.iecr.8b01189.

28 H. Miyagawa, M. Misra, L. T. Drzal and A. K. Mohanty, Novel biobased nanocomposites from functionalized vegetable oil and organically-modified layered silicate clay, *Polymer*, 2005, **46**, 445–453, DOI: 10.1016/j.polymer.2004.11.031.

29 F. Zanetti, B. Alberghini, A. Marjanovi, N. Grahovac, D. Rajkovi, B. Kiprovski and A. Monti, *et al.*, Camelina, an ancient oilseed crop actively contributing to the rural renaissance in Europe. A review, *Agron. Sustainable Dev.*, 2021, **41**(2), DOI: 10.1007/s13593-020-00663-y.

30 A. Slavova-Kazakova, M. Marcheva, S. Taneva and S. Momchilova, Oxidative Stability of the Oil from Camelina (Camelina sativa L.) Seeds: Effects of Ascorbyl Palmitate Concentrations, *Seeds*, 2025, **4**, 38.

31 M. Arshad, A. K. Mohanty, R. Van Acker, R. Riddle, J. Todd and H. Khalil, *et al.*, Valorization of camelina oil to biobased materials and biofuels for new industrial uses: a review, *RSC Adv.*, 2022, **12**, 27230–27245, DOI: 10.1039/d2ra03253h.

32 M. Arshad, S. Shankar, A. K. Mohanty, J. Todd, R. Riddle and R. Van Acker, *et al.*, Improving the Barrier and Mechanical Properties of Paper Used for Packing Applications with Renewable Hydrophobic Coatings Derived from Camelina Oil, *ACS Omega*, 2024, **9**, 19786–19795, DOI: 10.1021/acsomega.3c07213.

33 M. Safder, M. Arshad, F. Temelli and A. Ullah, Biocomposites from spent hen derived lipids grafted on CNC and reinforced with nanoclay, *Carbohydr. Polym.*, 2022, **281**, 119082, DOI: 10.1016/j.carbpol.2021.119082.

34 ASTM INTERNATIONAL, Standard Test Method for Tensile Properties of Plastics (ASTM D638), vol. 08, 2014.

35 ASTM INTERNATIONAL, Standard Test Methods for Flexural Properties of Unreinforced and Reinforced Plastics and Electrical Insulating Materials. D790. Annu B ASTM Stand 2002, pp. 1–12, DOI: 10.1520/D0790-17.2.

36 ASTM Standard D256, Standard Test Methods for Determining the Izod Pendulum Impact Resistance of Plastics, ASTM Int 2010, DOI: 10.1520/D0256-24.2.

37 Q. V. Bach, C. M. Vu, H. T. Vu, T. Hoang, T. V. Dieu and D. D. Nguyen, Epoxidized soybean oil grafted with CTBN as a novel toughener for improving the fracture toughness and mechanical properties of epoxy resin, *Polym. J.*, 2020, **52**, 345–357, DOI: 10.1038/s41428-019-0275-3.

38 M. B. Mahadi, I. S. Azmi, M. A. Ahmad, N. H. Rahim and M. J. Jalil, Catalytic epoxidation of sunflower oil derived by linoleic acid via in situ peracid mechanism, *Biomass Convers. Biorefin.*, 2025, **15**(6), 9505–9512, DOI: 10.1007/s13399-024-05658-3.

39 B. Balanuca, R. Stan, A. Lungu, E. Vasile and H. Iovu, Hybrid networks based on epoxidized camelina oil, *Des. Monomers Polym.*, 2017, **20**, 10–17, DOI: 10.1080/15685551.2016.1231031.

40 V. S. Giita Silverajah, N. A. Ibrahim, N. Zainuddin, W. M. Z. Wan Yunus and H. A. Hassan, Mechanical, thermal and morphological properties of poly(lactic acid)/epoxidized palm olein blend, *Molecules*, 2012, **17**, 11729–11747, DOI: 10.3390/molecules171011729.

41 B. W. Chieng, N. A. Ibrahim, Y. Y. Then and Y. Y. Loo, Epoxidized vegetable oils plasticized poly(lactic acid)

biocomposites: Mechanical, thermal and morphology properties, *Molecules*, 2014, **19**, 16024–16038, DOI: 10.3390/molecules191016024.

42 M. Bouti, R. Irinislimane and N. Belhaneche-Bensemra, Properties Investigation of Epoxidized Sunflower Oil as Bioplasticizer for Poly (Lactic Acid), *J. Polym. Environ.*, 2022, **30**, 232–245, DOI: 10.1007/s10924-021-02194-3.

43 B. Films, Epoxidized Soybean Oil Toughened Poly(lactic acid)/Lignin-g-Poly(lauryl methacrylate) Bio-Composite Films with Potential Food Packaging Application, *Polymers*, 2024, 16.

44 P. Siudem, A. Zielińska and K. Paradowska, Application of 1H NMR in the study of fatty acids composition of vegetable oils, *J. Pharm. Biomed. Anal.*, 2022, **212**, 1–8, DOI: 10.1016/j.jpba.2022.114658.

45 E. Alexandri, R. Ahmed, H. Siddiqui, M. I. Choudhary, C. G. Tsiafoulis and I. P. Gerothanassis, High resolution NMR spectroscopy as a structural and analytical tool for unsaturated lipids in solution, *Molecules*, 2017, 22, DOI: 10.3390/molecules22101663.

46 G. Çayli, S. Cekli and C. P. Uzunoğlu, Synthesis, photopolymerization and evaluation of electrical properties of epoxidized castor oil-based acrylates, *Polym. Bull.*, 2024, **81**, 13289–13304, DOI: 10.1007/s00289-024-05349-z.

47 T. Akintayo Emmanuel, O. Akintayo Cecilia, I. O. Oluwaleye, O. Ajaja and S. Beuermann, Synthesis and characterization of azidated Adenopus breviflorus benth seed oil, *Green Chem. Lett. Rev.*, 2020, **13**, 115–126, DOI: 10.1080/17518253.2020.1737251.

48 N. T. Thuy and P. N. Lan, Investigation of the impact of two types of epoxidized vietnam rubber seed oils on the properties of polylactic acid, *Adv. Polym. Technol.*, 2021, 2021, DOI: 10.1155/2021/6698918.

49 M. Maiza, M. T. Benaniba, G. Quintard and V. Massardier-Nageotte, Biobased additive plasticizing Polylactic acid (PLA), *Polimeros*, 2015, **25**, 581–590, DOI: 10.1590/0104-1428.1986.

50 Y. Farrag, L. Barral, O. Gualillo, D. Moncada, M. Rico and R. Bouza, Effect of Different Plasticizers on Thermal, Crystalline, and Permeability Properties, *Polymers*, 2022, 14.

51 D. Li, Y. Jiang, S. Lv, X. Liu, J. Gu and Q. Chen, *et al.*, Preparation of plasticized poly (lactic acid) and its influence on the properties of composite materials, *PLoS One*, 2018, **13**, 1–15, DOI: 10.1371/journal.pone.0193520.

52 M. Bocqué, C. Voirin, V. Lapinte, S. Caillol and J. J. Robin, Petro-based and bio-based plasticizers: Chemical structures to plasticizing properties, *J. Polym. Sci., Part A: Polym. Chem.*, 2016, **54**, 11–33, DOI: 10.1002/pola.27917.

53 Z. Eslami, S. Elkoun, M. Robert and K. Adjallé, A Review of the Effect of Plasticizers on the Physical and Mechanical Properties of Alginate-Based Films, *Molecules*, 2023, 28, DOI: 10.3390/molecules28186637.

54 J. Guo, J. Wang, Y. He, H. Sun, X. Chen and Q. Zheng, *et al.*, Triply biobased thermoplastic composites of polylactide/succinylated lignin/epoxidized soybean oil, *Polymers*, 2020, 12, DOI: 10.3390/polym12030632.

55 S. Wasti, E. Triggs, R. Farag, M. Auad, S. Adhikari and D. Bajwa, *et al.*, Influence of plasticizers on thermal and mechanical properties of biocomposite filaments made from lignin and polylactic acid for 3D printing, *Composites, Part B*, 2021, 205, DOI: 10.1016/j.compositesb.2020.108483.

56 P. H. Daniels, A brief overview of theories of PVC plasticization and methods used to evaluate PVC-plasticizer interaction, *J. Vinyl Addit. Technol.*, 2009, **15**, 219–223, DOI: 10.1002/vnl.20211.

57 J. Xie, K. Gu, Y. Zhao, J. Yao, X. Chen and Z. Shao, Enhancement of the Mechanical Properties of Poly(lactic acid)/Epoxidized Soybean Oil Blends by the Addition of 3-Aminophenylboronic Acid, *ACS Omega*, 2022, **7**, 17841–17848, DOI: 10.1021/acsomega.2c01102.

58 T. H. Zhao, W. Q. Yuan, Y. D. Li, Y. X. Weng and J. B. Zeng, Relating Chemical Structure to Toughness via Morphology Control in Fully Sustainable Sebacic Acid Cured Epoxidized Soybean Oil Toughened Polylactide Blends, *Macromolecules*, 2018, **51**, 2027–2037, DOI: 10.1021/acs.macromol.8b00103.

59 A. Orue, A. Eceiza and A. Arbelaiz, Preparation and characterization of poly(lactic acid) plasticized with vegetable oils and reinforced with sisal fibers, *Ind. Crops Prod.*, 2018, **112**, 170–180, DOI: 10.1016/j.indcrop.2017.11.011.

60 Y. B. Tee, R. A. Talib, K. Abdan, N. L. Chin, R. K. Basha and K. F. M. Yunos, Toughening Poly(Lactic Acid) and Aiding the Melt-compounding with Bio-sourced Plasticizers, *Agric. Agric. Sci. Procedia*, 2014, **2**, 289–295, DOI: 10.1016/j.aaspro.2014.11.041.

61 C. Lazaro-Hdez, A. P. Valerga, J. Gomez-Carturla, L. Sanchez-Nacher, T. Boronat and J. Ivorra-Martinez, Optimization of the ductile properties of poly(lactic acid) (PLA) using green citrate-based plasticizers and itaconic anhydride grafted PLA (PLA-g-IA), *Int. J. Biol. Macromol.*, 2025, **307**, 142034, DOI: 10.1016/j.ijbiomac.2025.142034.

62 B. W. Chieng, N. A. Ibrahim, Y. Y. Then and Y. Y. Loo, Mechanical, thermal, and morphology properties of poly (lactic acid) plasticized with poly (ethylene glycol) and epoxidized palm oil hybrid plasticizer, *Polym. Eng. Sci.*, 2016, **56**, 1169–1174, DOI: 10.1002/pen.

63 L. Najera-Losada, P. C. Narváez-Rincón, A. Orjuela, J. Gomez-Caturla, O. Fenollar and R. Balart, Plasticization of Polylactide Using Biobased Epoxidized Isobutyl Esters Derived from Waste Soybean Oil Deodorizer Distillate, *J. Polym. Environ.*, 2025, **33**, 125–144, DOI: 10.1007/s10924-024-03415-1.

64 R. Tejada-Oliveros, R. Balart, J. Ivorra-Martinez, J. Gomez-Caturla, N. Montanes and L. Quiles-Carrillo, Improvement of Impact Strength of Polylactide Blends with a Thermoplastic Elastomer Compatibilized with Biobased Maleinized Linseed Oil for Applications in Rigid Packaging, *Molecules*, 2021, **26**, 240, DOI: 10.3390/MOLECULES26010240.

65 H. Gao and T. Qiang, Fracture surface morphology and impact strength of cellulose/PLA composites, *Materials*, 2017, **10**, 1–11, DOI: 10.3390/ma10060624.

66 D. K. Pradhan, B. K. Samantaray, R. N. P. Choudhary and A. K. Thakur, Effect of plasticizer on structure - Property relationship in composite polymer electrolytes, *J. Power Sources*, 2005, **139**, 384–393, DOI: 10.1016/j.jpowsour.2004.05.050.

67 Y. F. Minale, I. Gajdoš, P. Štefčák, T. Szabó, A. P. Kovács, A. Á. Major and K. Marossy, *et al.*, Mechanical Properties of PVC/TPU Blends Enhanced with a Sustainable Bio-Plasticizer, *Sustainability*, 2025, **17**(5), 2033, DOI: 10.3390/su17052033.